

Available online at www.sciencedirect.com**ScienceDirect**

Procedia Engineering 102 (2015) 1656 – 1666

**Procedia
Engineering**www.elsevier.com/locate/procedia

The 7th World Congress on Particle Technology (WCPT7)

Hindered Settling Velocity & Structure formation during particle settling by Direct Numerical Simulation

Ali Abbas Zaidi^{a*}, Takuya Tsuji^a, Toshitsugu Tanaka^{a*}*Department of Mechanical Engineering Osaka University, Suita 565-0871, Japan*

Abstract

Direct numerical simulation is used to study the dynamics of particle settling for Reynolds number from 0.1 to 50 and solid volume fraction from single particle to 0.4. The principle investigations are the effects of Reynolds number and solid volume fraction on average settling velocity, velocity fluctuations and particles structuring during settling. It is observed that average settling velocity deviates from the well-known power law for dilute suspension and moderate range of Reynolds number. Moreover, the increase of velocity fluctuations with domain size saturates and becomes about constant for moderate range of Reynolds numbers in contrast to low Reynolds number in which the fluctuations keep increasing. These behaviors are due to the separated particle pairs which are formed due to inter-particle wake interactions. As the solid volume fraction increases, the smaller inter-particle distances diminish the wake effects and corresponding particle structures.

© 2015 The Authors. Published by Elsevier Ltd. This is an open access article under the CC BY-NC-ND license

(<http://creativecommons.org/licenses/by-nc-nd/4.0/>).

Selection and peer-review under responsibility of Chinese Society of Particuology, Institute of Process Engineering, Chinese Academy of Sciences (CAS)

Keywords: Hindered settling velocity; Velocity fluctuations; Particle structuring; Particle settling; Direct numerical simulations

1. Introduction

The settling or sedimentation of particles in fluid is a common phenomenon both in nature and various industrial processes. Some of the particular applications areas are separating dirt or crystals from liquids, separating dust particles from air-streams, settling of micro-organisms and migration of micro-scale particles [1]. The suspension

* Corresponding author. Tel.: +81-6-6879-7316; fax: +81-6-6879-7316.

E-mail address: ali@cf.mech.eng.osaka-u.ac.jp

tanaka@mech.eng.osaka-u.ac.jp

fluid can be air or water and the body force which drives the suspended particles can be gravity, electric or magnetic forces. In the case of non-Brownian settling process in which the hydrodynamic interactions between particles are the principle forces, particles develop structures which affect the settling characteristics e.g. average settling velocity and fluid velocity fluctuations. These particle structures are constantly changing which makes the understanding of settling difficult.

The advancement in computational resources made particle resolved direct numerical simulations (DNS) possible. DNS gives better control over problem setup in comparison with experiments without the need of closure relations. Some of the problems associated with the experiments are scatter in the size of particles, calculation of average settling velocity for dilute suspensions and tracking of large number of particles during settling. DNS can solve these problems efficiently and if care is taken in the selection of grid, it is capable of giving reliable and accurate results. Thus DNS is used in the current paper for the investigations of settling process.

From fundamental viewpoint of settling, investigations on the mean settling velocity and velocity fluctuations are important. In literature, for low ranges of Reynolds number (i.e. Stokes flow regime) there are reasonable number of studies both by experiments and simulations [2-5]. However for moderate ranges of Reynolds number i.e. when the fluid inertia breaks the fore and aft symmetry of fluid around particles, studies are few [1,6,7] and further investigations are possible. The main reason for smaller number of simulation studies for moderate ranges of Reynolds number is the increase of computational cost due to the requirement of fine grid. The objectives of this paper is to investigate the effects of Reynolds number and solid volume fraction on average settling velocity, velocity fluctuations and particle structures which are formed during settling. The Reynolds number which is studied in the simulation ranges from 0.1 to 50 and the studied ranges of solid volume fraction varies from single sphere to 0.4. This range of Reynolds number reasonably covers the fluid inertia regime without large increase in the computational cost.

The organization of this paper is as follows: after introduction a brief overview of formulation is given. It will be followed by simulation setup, after that results are presented and physics is described. At the end paper is concluded by key findings and acknowledgements.

Nomenclature

a	Parameter for classifying particle clusters
d_p	Particle diameter
dx	Grid size
f	Friction coefficient
F_n	Normal Component of force on particle-particle collision
F_t	Tangential component of force on particle-particle collision
f_p	Forcing term
$g(r)$	Radial distribution function at an inter-particle distance r
\mathbf{G}	Relative particle velocity vector between colliding particles
K	Spring constant
L	Length of the side of cubic domain
n	Time step
$n(r)$	Number of particles in the shell of radius r
p	Fluid pressure
\mathbf{r}	Unit vector from the center of rotation to the surface
\mathbf{r}_i	Position vector of particle i
\mathbf{r}_j	Position vector of particle j
t	time
t'	Stokes time
Re	Reynolds number
St	Stokes number
\mathbf{u}	Fluid-particle volume-weighted velocity
$\tilde{\mathbf{u}}$	Predicted velocity

\mathbf{u}_f	Fluid velocity
\mathbf{u}_p	Velocity inside the solid particle
U_s	Terminal velocity of particle
\mathbf{v}_p	Velocity of particle center
V_p	Average particle velocity
V_{p1}	Volume of cubewith sides equal to the sphere diameter
$\boldsymbol{\omega}_p$	Angular velocity of particle rotation
x, y, z	Cartesian coordinate directions
α	Volume fraction of particles
ρ	Fluid density
ρ_d	Particle density
ρ^n	Number density
ν	Kinematic viscosity
μ	Viscosity
δ	Particle overlap during collision
η	Damping coefficient
φ	Solid volume fraction
Δt	Time step
Δr	Shell radius

2. Formulation

In simulations, immersed boundary method is used for fluid-particle interactions and discrete element method is used for particle-particle interactions.

2.1. Immersed Boundary Method (IBM)

In the present simulations body force type IBM by Kajishima et al. [8] is used. IBM lies in the particle resolved type DNS in which grid size is smaller than the size of particles and the fluid flow is calculated by assuming the fluid occupies the entire flow field. The effect of particles is expressed by a body force into the momentum equation of fluid which constrains the no slip boundary condition at the particles surface. So the equations of continuity and incompressible Navier-Stokes equation without gravity effects is given by:

$$\nabla \cdot \mathbf{u}_f = 0 \quad (1)$$

$$\frac{\partial \mathbf{u}_f}{\partial t} + \mathbf{u}_f \cdot \nabla \mathbf{u}_f = \nu \nabla^2 \mathbf{u}_f - \frac{\nabla p}{\rho} \quad (2)$$

For performing the numerical integration fluid-particle volume-weighted velocity (\mathbf{u}) is defined by:

$$\mathbf{u} = \alpha \mathbf{u}_p + (1 - \alpha) \mathbf{u}_f \quad (3)$$

α takes the value zero for fluid and one for particle and in the range of zero to one at the interface. The velocity inside the solid particle is defined by:

$$\mathbf{u}_p = \mathbf{v}_p + \boldsymbol{\omega}_p \times \mathbf{r} \quad (4)$$

For the case of no slip and no permeable conditions at the interface ($\mathbf{u}_f = \mathbf{u}_p$), the continuity restriction should also be satisfied for \mathbf{u} . The momentum equation of fluid in IBM is given by:

$$\frac{\partial \mathbf{u}}{\partial t} + \mathbf{u} \cdot \nabla \mathbf{u} = \nu \nabla^2 \mathbf{u} - \frac{\nabla p}{\rho} + \mathbf{f}_p \quad (5)$$

where \mathbf{f}_p is the force to modify the flow predicted as if the field is occupied by fluid to the velocity defined by Eq.

(3).The time-marching of Eq. (5) consists of two steps, in the first step we predict the velocity by using Eq.(2)without taking into account of \mathbf{f}_p .

$$\tilde{\mathbf{u}} = \mathbf{u}_n + \Delta t \left(-\frac{\nabla p}{\rho} - \mathbf{u} \cdot \nabla \mathbf{u} + \nu \nabla^2 \mathbf{u} \right) \quad (6)$$

In the second step, $\tilde{\mathbf{u}}$ is constrained to the volume-weighted velocity by the forcing term given by:

$$\mathbf{f}_p = \alpha(\mathbf{u}_p - \tilde{\mathbf{u}})/\Delta t \quad (7)$$

The fluid force and fluid moment on a particle are calculated by the volume integral equations Eq. (8) and Eq.(9).

$$\mathbf{F}_f = -\rho \int_{V_p} \mathbf{f}_p dv \quad (8)$$

$$\mathbf{M}_f = -\rho \int_{V_p} \mathbf{r} \times \mathbf{f}_p dv \quad (9)$$

A general difficulty with IBM is its inability to resolve the fluid force when a pair of particles approach each other and the separation distance becomes comparable to or smaller than the grid spacing. This may affect the accuracy of results. To overcome this problem, rather than using fine mesh resolutions to resolve the flows in small gaps, we have used the analytical results for the lubrication force to describe these short range interactions. The detail of this method can be found in the paper of Simeonov and Calantoni [9]. The lubrication force between the two spheres which are going to collide diverges as the separation distance between the two spheres approaches zero. However in real applications this divergence can be removed due to particle roughness. According to Simeonov and Calantoni [9] the lubrication force should be equal to zero if the ratio of inter-particle distance to particle diameter becomes less than the $O(10^{-4})$.

2.2. Discrete Element Method (DEM)

In DEM by Cundall and Strack [10] the contact force between two particles or particle and wall is modeled by springs, dashpots and friction slider. The contact force is divided into normal component \mathbf{F}_n and tangential component \mathbf{F}_t .

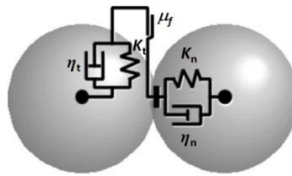


Fig. 1. DEM model.

$$\mathbf{F}_n = (-K_n \delta_n - \eta_n \mathbf{G} \cdot \mathbf{n}) \mathbf{n} \quad (10)$$

$$\mathbf{F}_t = (-K_t \delta_t - \eta_t G_{ct}) \mathbf{t} \quad (11)$$

$$\text{If } |\mathbf{F}_t| > f |\mathbf{F}_n| \quad (12)$$

$$\mathbf{F}_t = -f |\mathbf{F}_n| \mathbf{t} \quad (13)$$

Subscripts t indicates tangential and n indicates normal direction respectively. \mathbf{G} is the relative particle velocity to the collision partner, \mathbf{n} and \mathbf{t} are the normal and tangential unit vector at the contact point.

For time marching of velocities and displacements of particles, we have used second order Adams-Bashforth and second order Crank-Nicolson schemes respectively.

3. Simulation Setup

In the simulations, randomly arranged particles are allowed to settle under gravity in cubic domain with length L in x , y and z directions. The boundary condition is periodic and volume flow rate of fluid within the domain is zero to replicate the unbounded suspension. The gravity direction during particles settling is taken to be at an angle between 10-30 degrees from the axis of the computational domains to prevent the particles from interacting with their own wakes. Water is used as fluid and the range of Reynolds number studied in simulations are $Re=0.1, 1, 10, 20, 30, 40$ and 50 . Magnitude of gravity is used to control Reynolds number which is defined as:

$$Re = \frac{U_s d_p}{\nu} \quad (14)$$

The number of particles in the domain is selected in such a way to get desired solid volume fractions. The solid volume fractions studied in simulations are from single particle to 0.4 . The parameters of DEM solver used in the simulations are given by:

Table 1. Parameters of DEM.

Parameter	Value
Coefficient of Restitution [-]	0.9
Normal Spring Constant [N/m]	800
Coefficient of Particle Friction [-]	0.25

The results presented in the next section are ensemble averaged for three independent simulations for each Reynolds number and solid volume fraction. In particle settling simulation selection of proper grid is important so careful attention is paid for the selection of grid. Table 2 shows the grid resolutions used in the simulations. All the results presented in next section are time averaged for about 300-500 Stokes time. ($t' = tU_s/d_p$)

Table 2. Grid resolution used in simulations.

Case	d_p/dx
$Re \leq 1$ $\phi \leq 0.1$	8
$Re \leq 1$ $\phi > 0.1$	16
$Re > 1$ $\phi \leq 0.1$	16
$Re > 1$ $\phi > 0.1$	24

4. Results & Discussion

4.1. Hindered Settling Velocity

In literature [11, 12] it is evidenced the mean settling velocity of mono disperse spheres is less than the terminal velocity of an isolated sphere due to inter-particle interactions. In chemical engineering applications, there is a famous mathematical relation developed by Richardson & Zaki (R&Z) [13] based on their experimental results. It is given by:

$$U = \frac{V_p}{U_s} = (1 - \phi)^{n_e} \quad (15)$$

The equation of n_e proposed by R&Z is:

$$n_e = \begin{cases} 4.65 & Re < 0.2 \\ 4.4Re^{-0.03} & 0.2 < Re < 1 \\ 4.4Re^{-0.1} & 1 < Re < 500 \\ 2.4 & Re > 500 \end{cases} \quad (16)$$

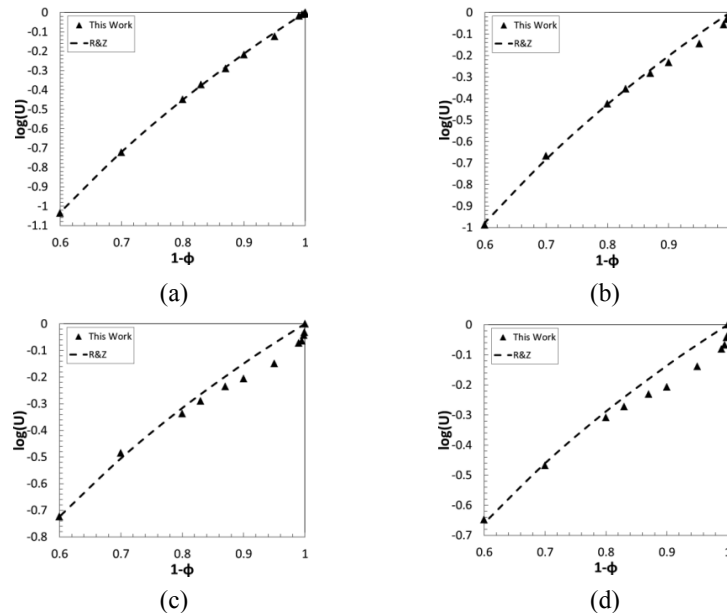


Fig.2.Hindered Settling Velocity as function of $(1-\phi)$ (a) $Re=0.1$ (b) $Re=1$ (c) $Re=20$ (d) $Re=50$.

In simulations the above mentioned relation is used for comparison and shown in Fig.2. The terminal velocity is obtained by allowing a single particle to settle in the domain. For average particle velocity, it is observed that the domain size has negligible effect. Thus in the calculation of average settling velocity $L/d_p=10$ is used.

It can be seen that R&Z relation reasonably agrees with the simulations data for low ($Re \approx 0.1$) and moderate Reynolds number ($Re > 0.1$) & dense suspension ($\phi \geq 0.2$). However for moderate Reynolds number ($Re > 0.1$) and dilute suspension ($\phi \leq 0.1$) simulation results show deviation and it keeps on increasing with the increase in Reynolds number and decrease in solid volume fraction. The reason for this deviation will be explained later.

4.2. Velocity Fluctuations

When the particles settle under gravity, all the particles are not settled with the same averaged velocity but develop some deviations and fluctuations about the mean or average settling velocity. These deviations are called velocity fluctuations. The origin of these fluctuations is the hydrodynamic interactions between particles and is the source of mixing. Particle velocity fluctuations induce fluid velocity fluctuations and turbulent kinetic energy. For low range of Reynolds number, Caflish and Luke [14] proposed that the hydrodynamic interactions among randomly distributed sedimenting particles lead to linear growth of the particle velocity fluctuations with the size of the suspension. Later numerical simulations [2, 3] subject to periodic boundary conditions and low Reynolds number benchmarked the studies done by Caflish and Luke [14]. Recently, Segre [15] explained by experiments that there is a characteristic length of vortices above which the effect of domain size on velocity fluctuations becomes negligible. In the range of Oseen-wake interactions and dilute suspension; Koch [16] based on his

theoretical study showed that wakes around particles should screen the velocity fluctuations with domain size. In this section, we will discuss the effect of domain size on velocity fluctuations for both low and moderate Reynolds number, i.e. $Re=1, 50$. In this section, only $\phi=0.01$ is selected for studying the velocity fluctuations, similar trend is observed for higher solid volume fractions. For studying velocity fluctuations, variance of particle and fluid velocity is used and it is non-dimensionalized by the square of terminal velocity of single particle. The domain sizes studied for both cases is $L/d_p=10, 15, 25, 35$ and 50 . Fig.3 shows the velocity fluctuations in vertical and horizontal direction.

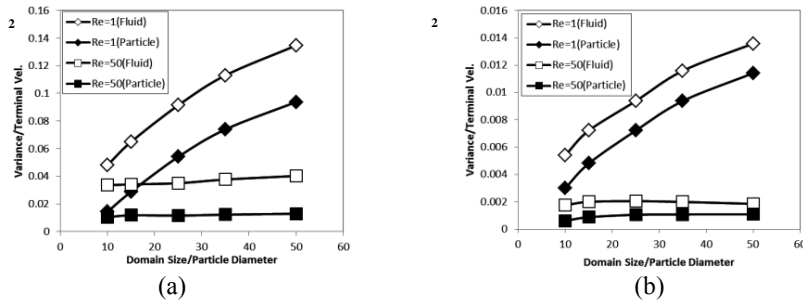


Fig.3. Velocity fluctuations for $\phi=0.01$ and $Re=1, 50$ (a) Vertical Direction (b) Horizontal Direction.

It can be seen in Fig.3 that for $Re=1$, the velocity fluctuations keep increasing with the domain size. However for $Re=50$ the increase of velocity fluctuations with domain size is much less pronounced. Moreover, comparison of vertical and horizontal velocity fluctuations indicates that anisotropy is still strong. Particle velocity fluctuations in the vertical direction is greater than the horizontal ones (about 7.5 times for $Re=1$ and 12 times for $Re=50$) indicating the influence of forcing due to gravity. Another important point is that the fluid velocity variance is larger than the particle velocity variance. This may be due to the failure of particles to follow fluid motions on length scales equal to or smaller than the particle diameter. However the variation of fluid velocity fluctuations with domain size is about parallel to the variance of particle velocity for both Reynolds number. The physical reason for this behavior of velocity fluctuations will be explained later.

4.3. Structure Formation

When two particles settle under Stokes flow condition i.e. low Reynolds number the inter-particle distance remain fixed because of the absence of non-linear wake interactions between particles which give rise to long range velocity perturbations. However, when the Reynolds number increases the wakes from the leading particle affects the particle on the downstream side and lead to a phenomenon that is called drafting, kissing and tumbling [17]. In the case of large number of particles, these interactions become complex and lead to non-random particle structures. Experimentally these structures are difficult to visualize and classify especially for high solid volume fraction. Thus in literatures, most of the experimental studies are focused on two dimensions. Particle resolved DNS can keep track of all particles for long durations. In this article, for classifying the particle structures, we studied particle clusters and radial distribution function (RDF).

Cluster Analysis

Herrmann et al. [18] proposed a method for percolation problem on classifying particle clusters. Two particles are said to be in the same clusters when they are at a distance of ad_p from each other where a is the non-dimensional parameter.

$$|\mathbf{r}_i - \mathbf{r}_j| \leq a(d_p) \quad (17)$$

a is the main parameter for classifying particle clusters and thus its value is critical. Xiong et al. [19] studied a and observed that their results remain qualitatively same by changing a from $1.05d_p$ to $1.2d_p$. As we studied both dilute and dense suspensions, thus this parameter should not be large otherwise for dense suspension all the

particles will be in the same cluster. We used $a=1.05$ for all ϕ because it worked well without changing the qualitative trend.

After steady state, percentage of particles acting as single particles and clusters of two, three and more than three particles is calculated.

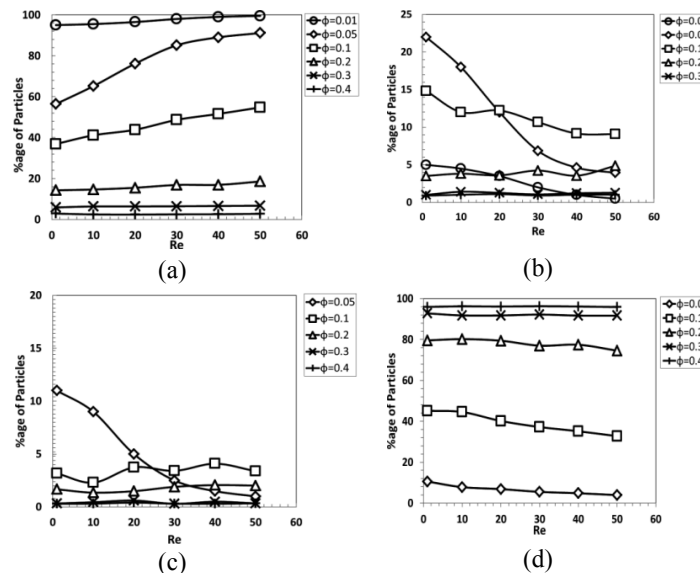


Fig.4. Percentage of particles participating in clusters of (a) Single particle size (b) Two particle size (c) Three particle size (d) More than three particle size.

For high solid volume fraction ($\phi \geq 0.3$) it can be seen that the effect of Reynolds number is negligible and the particle clustering is directly proportional to the solid volume fraction. This is in coherence with intuition, as the solid volume fraction increases the inter-particle distance decreases and hence large particle clusters are possible. However for relatively low solid volume fractions ($\phi \leq 0.2$), Reynolds number adversely affects the particle clustering. As an example for $\phi=0.01$ and $Re=50$ all the particles are separated and for $\phi=0.05$ the percentage of single particles increases from 56% to 91% for Reynolds number from 1 to 50.

Radial distribution function

Radial distribution function (RDF) gives the information of overall structures formed in suspension. It is defined by:

$$g(r) = \frac{n(r)}{4\pi\rho^n r^2 \Delta r} \quad (18)$$

A higher peak of RDF at some particular inter-particle separation shows higher probability of finding particle at that particular distance. Furthermore, RDF tends to the value of 1 at larger inter-particle distance showing number density equal to the bulk number density. For obtaining the overall structure this function is averaged over all the particles. For comparing with the RDF of hard spheres (HS), RDF calculated for Percus-Yevick equation [20] is also shown in Fig. 5. As an example RDF for $\phi=0.05$ and $\phi=0.2$ is shown for $Re=1, 20$ and 50 .

For $\phi=0.2$, the RDF for hard sphere distribution and all studied Reynolds numbers are quite identical. However for $\phi=0.05$, the particle distribution in settling is different from HS distribution. For $Re=1$, the particles show more close pairs with higher peaks of RDF at smaller shells. RDF changes both in magnitude of the peak value and the region where peak lies by increasing the Reynolds number. For longer inter-particle distance ($r/d_p \geq 3$), the particle distribution becomes random.

For studying the effect of domain size on RDF two cases have been studied $\phi=0.01$ and $Re=1$ and 50 . Like velocity fluctuations in the previous section RDF changes with the increase in domain size for $Re=1$. However for

$Re=50$ the effect of domain size on RDF is negligible.

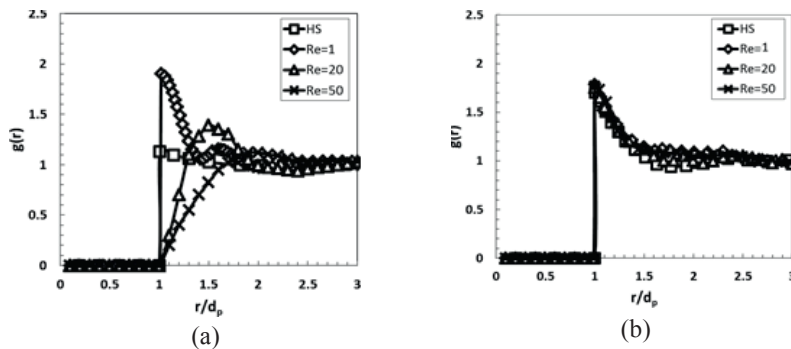


Fig.5. Radial Distribution Function for (a) $\phi=0.05$ (b) $\phi=0.2$.

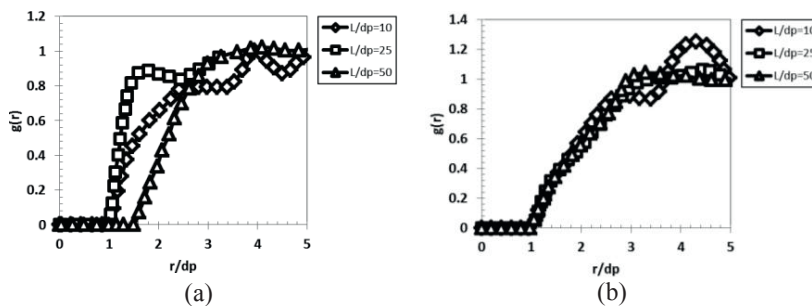


Fig.6. Radial Distribution Function for $\phi=0.01$ (a) $Re=1$ (b) $Re=50$.

4.4. Physics of particle settling

It has been observed in the previous sections that the Reynolds number affect the settling characteristics. Furthermore, increase in solid volume fraction diminishes the effects of Reynolds number. This is due to the particle structures which are formed due to Drafting-Kissing and tumbling (DKT) [17]. We will first explain this phenomenon in detail and then extend this concept for particle settling.

First it is necessary to understand about the variation in the flow structures around particles with the Reynolds number. For this we took a simple case in which a particle is fixed in a rectangular computational domain and flow is going in the direction perpendicular to horizontal plane. In this particular example we studied $Re=100, 250, 300$ and 450 . For very low Reynolds number ($Re < 0.1$) the wakes around the particles are very weak. As the Reynolds number increases particle develop axisymmetric attached vortex ring and it remain till about $Re \leq 200-250$. Further increase in the Reynolds number changes the axisymmetric wake structures to plane symmetric wakes till at about $Re > 300$ unsteady vortex shedding starts. Further increase in the Reynolds number changes the period and shape of vortices. This wake behaviour can be seen in Fig.7. For identifying wakes iso-surfaces of $\nabla^2 p = 1.5 \times 10^6$ is used.

Particle wakes are the regions of low drag for downstream particles. As the downstream particle experiences reduced drag it moves faster till it touches the leading particle which is called kissing. The approach phase of downstream particle is called drafting. Particles in the touching arrangement are unstable and try to separate and form horizontally separated pairs. This is called tumbling. All these three phases for two particles is shown in Fig.8 and 9. It can be visualized that DKT will have a large effect on particle settling. We observed that wakes for $Re \leq 0.2$ supports no DKT, for $0.2 \leq Re \leq 1$ wakes are strong enough to support DK and for about $Re > 1$ wakes becomes sufficiently strong to promote all the three phases of DKT. The frequency of DKT depends upon the Reynolds number i.e. the larger the Reynolds number more frequent will be DKT for particles.

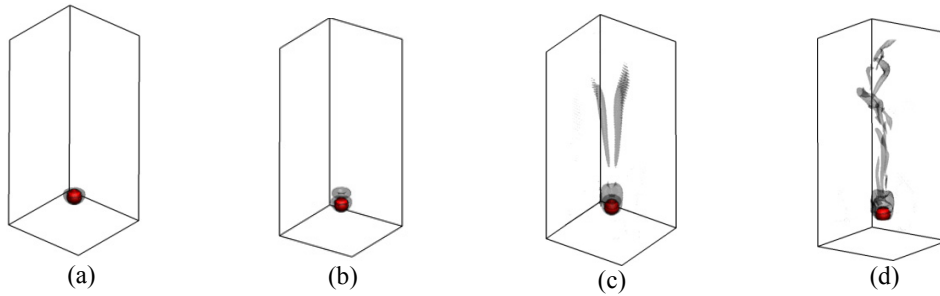


Fig. 7. Iso-surfaces of $\nabla^2 p = 1.5 \times 10^6$ around single sphere (a) $Re=100$ (b) $Re=250$ (c) $Re=300$ (d) $Re=450$.

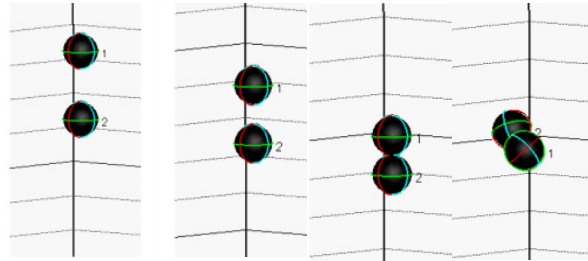


Fig. 8. Particle arrangements during DKT.

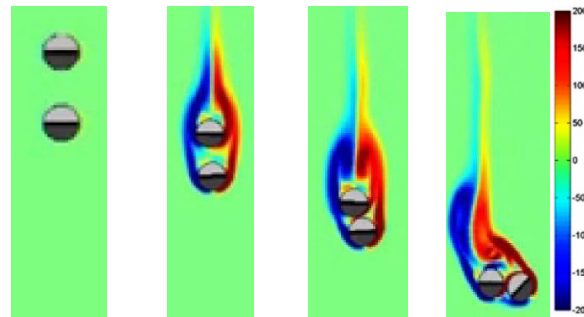


Fig. 9. Fluid vorticity during DKT.

It is observed in Section 4.3 that for dilute suspensions, separated particle pairs increases with increase in Reynolds number. It is due to the increase in the frequency of DKT which promoted horizontally separated pairs. In the case of dense suspensions, the smaller inter-particlespacing lead to diffused wake structures and smaller space for DKT to occur. The decrease in the average settling velocityfor dilute suspensions and $Re \geq 1$ in comparison with the relation of R&Z is due to increased drag on separated particle pairs. Furthermore, the saturation of velocity fluctuations with the domain size for $\phi=0.01$ and $Re=50$ and is due to reduction in the hydrodynamics interactions between separated particles due to DKT.

It is to be noted that all these statements are applicable only for relatively low stokes number suspensions i.e. liquid solid flows. Stokes number can be defined by:

$$St = \frac{\rho_d d_p^2}{18\mu t'} \quad (19)$$

In the studied cases, Stokes number is varied from $St=0.015-7$. Ma et al. [21, 22] studied DNS of high Stokes number gas-solid suspension. They proposed from their results that besides DKT the particle structuring in gas-solid flows is also controlled by minimization of gravitational potential of particles or minimization in local voidage and least resistance to gas flow in the suspension.

4. Conclusions

In this article, dynamics of settling of particles in periodic domain is investigated by using Immersed Boundary Method and Discrete Element Method. The studied Reynolds number is in the range of 0.1-50 and solid volume fraction ranges from single sphere to 0.4. It is observed that the average settling velocity of particles deviate from R&Z relation for dilute suspension and higher range of Reynolds number. Moreover the increase of velocity fluctuations with domain size is smaller for moderate Reynolds number. Particle structuring analysis showed that these are due to DKT which leads to horizontally separated particles. As the solid volume fraction increases the smaller inter-particle spacing diminishes the effects of moderate Reynolds number.

Acknowledgements

We would like to acknowledge Cybermedia Center, Osaka University and Center for Computing & Media Studies, Kyoto University for providing computational resources.

References

- [1] E. Climent, M.R. Maxey, Numerical simulations of random suspensions at finite Reynolds numbers, *Int J Multiphase Flow* 29 (2003) 579-601.
- [2] A.J.C. Ladd, Sedimentation of homogeneous suspensions of non-Brownian spheres, *Phys Fluids* 9 (1997) 491-499.
- [3] A.J.C. Ladd, R. Verberg, Lattice-Boltzmann simulations of particle-fluid suspensions, *J. Stat. Phys.* 104 (2001) 1191-1251.
- [4] H. Nicolai, E. Guazzelli, Effect of the Vessel Size on the Hydrodynamic Diffusion of Sedimenting Spheres, *Phys. Fluids* 7 (1995) 3-5.
- [5] H. Nicolai, Y. Peysson, E. Guazzelli, Velocity fluctuations of a heavy sphere falling through a sedimenting suspension, *Phys. Fluids* 8 (1996) 855-862.
- [6] X.L. Yin, D.L. Koch, Hindered settling velocity and microstructure in suspensions of solid spheres with moderate Reynolds numbers, *Phys. Fluids* 19 (2007) 535-550.
- [7] X.L. Yin, D.L. Koch, Velocity fluctuations and hydrodynamic diffusion in finite-Reynolds-number sedimenting suspensions, *Phys. Fluids* 20 (2008) 550-575.
- [8] T. Kajishima, S. Takiguchi, H. Hamasaki, Y. Miyake, Turbulence structure of particle-laden flow in a vertical plane channel due to vortex shedding, *J. Smol. Int. J. B-Fluid* T 44 (2001) 526-535.
- [9] J.A. Simeonov, J. Calantoni, Modeling mechanical contact and lubrication in Direct Numerical Simulations of colliding particles, *Int J Multiphase Flow* 46 (2012) 38-53.
- [10] P.A. Cundall, O.D.L. Strack, Discrete Numerical-Model for Granular Assemblies, *Geotechnique* 29 (1979) 47-65.
- [11] J.M. Ham, G.M. Homay, Hindered Settling and Hydrodynamic Dispersion in Quiescent Sedimenting Suspensions, *Int J Multiphase Flow* 14 (1988) 533-546.
- [12] M.A. Alnaafa, M.S. Selim, Sedimentation of Monodisperse and Bidisperse Hard-Sphere Colloidal Suspensions, *AIChE J.* 38 (1992) 1618-1630.
- [13] J. Richardson, W.N. Zaki, Sedimentation and fluidization: Part 1, *Trans. Inst. Chem. Eng.* 32 (1954) 35-53.
- [14] R.E. Caflisch, J.H.C. Luke, Variance in the Sedimentation Speed of a Suspension, *Phys Fluids* 28 (1985) 759-760.
- [15] P.N. Segre, Origin of stability in sedimentation, *Phys Rev Lett* 89 (2002) 435-440.
- [16] D.L. Koch, Hydrodynamic Diffusion in Dilute Sedimenting Suspensions at Moderate Reynolds-Numbers, *Phys Fluids a-Fluid* 5 (1993) 1141-1155.
- [17] A.F. Fortes, D.D. Joseph, T.S. Lundgren, Nonlinear Mechanics of Fluidization of Beds of Spherical-Particles, *J Fluid Mech* 177 (1987) 467-483.
- [18] H.J. Herrmann, D.C. Hong, H.E. Stanley, Backbone and Elastic Backbone of Percolation Clusters Obtained by the New Method of Burning, *J Phys a-Math Gen* 17 (1984) L261-L266.
- [19] Q.G. Xiong, B. Li, F.G. Chen, J.S. Ma, W. Ge, J.H. Li, Direct numerical simulation of sub-grid structures in gas-solid flow-GPU implementation of macro-scale pseudo-particle modeling, *Chem Eng Sci* 65 (2010) 5356-5365.
- [20] E. Thiele, Equation of State for Hard Spheres, *J Chem Phys* 39 (1963) 474-482.
- [21] J.S. Ma, W. Ge, Q.G. Xiong, J.W. Wang, J.H. Li, High-resolution simulation of gas-solid suspension using macro-scale particle methods, *Chem Eng Sci* 61 (2006) 7096-7106.
- [22] J.S. Ma, W. Ge, Q.G. Xiong, J.W. Wang, J.H. Li, Direct numerical simulation of particle clustering in gas-solid flow with a macro-scale particle method, *Chem Eng Sci* 64 (2009) 43-51.